

Expanded View Figures

Figure EV1. BGL3 directly binds BARD1 and PARP1 in living cells.

- A Schematic overview of RAP-MS.
- B RT-PCR products of RNA antisense captured lncRNAs were analyzed on an agarose gel. Ladder, 1 kb (Maker1) and 100 bp (Maker2) DNA ladder. F1: BGL3 DNA fragment 1–970 bp, F2: BGL3 DNA fragment 970–2,016 bp, F3: BGL3 DNA fragment 1,905–2,650 bp, F4: BGL3 DNA fragment 3,181–3,696 bp.
- C LncRNA being pulled down in the “BGL3 antisense group” (BGL3 group) and the control group (RMRP group) was examined by qRT-PCR using three different primers. P1: primer1, P2: primer2, P3: primer3. Data were presented as mean \pm SD of three biological replicates and analyzed by two-tailed Student’s *t*-test, ***P* < 0.01.
- D Overlap of non-redundant quantified proteins captured by BGL3 in three biological replicates.
- E Pairwise correlations of protein intensity between replicate experiments. The Pearson correlation coefficient is indicated.
- F BGL3-interacting proteins were grouped based on cellular component and biological process pathways by GO analysis.

Source data are available online for this figure.

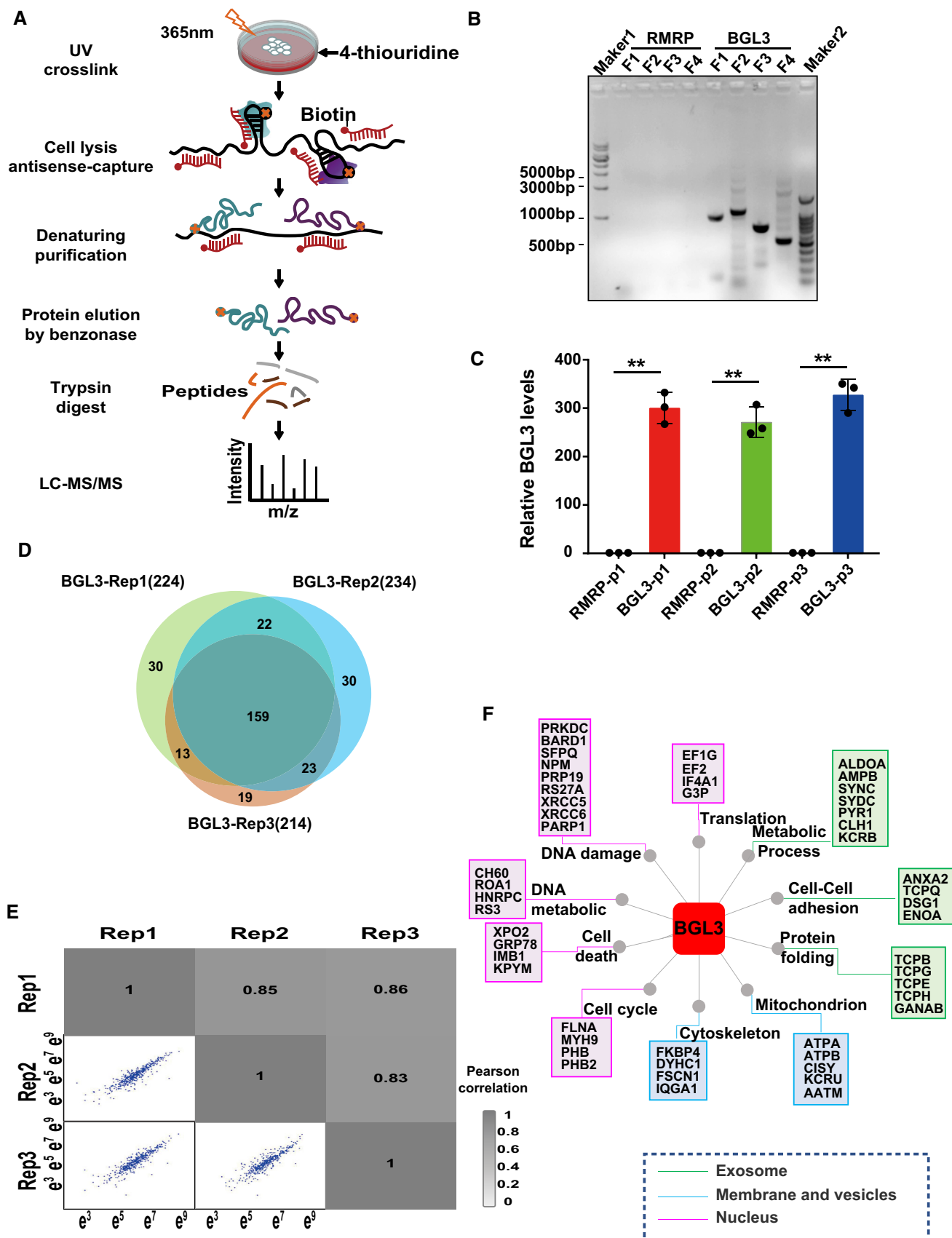


Figure EV1.

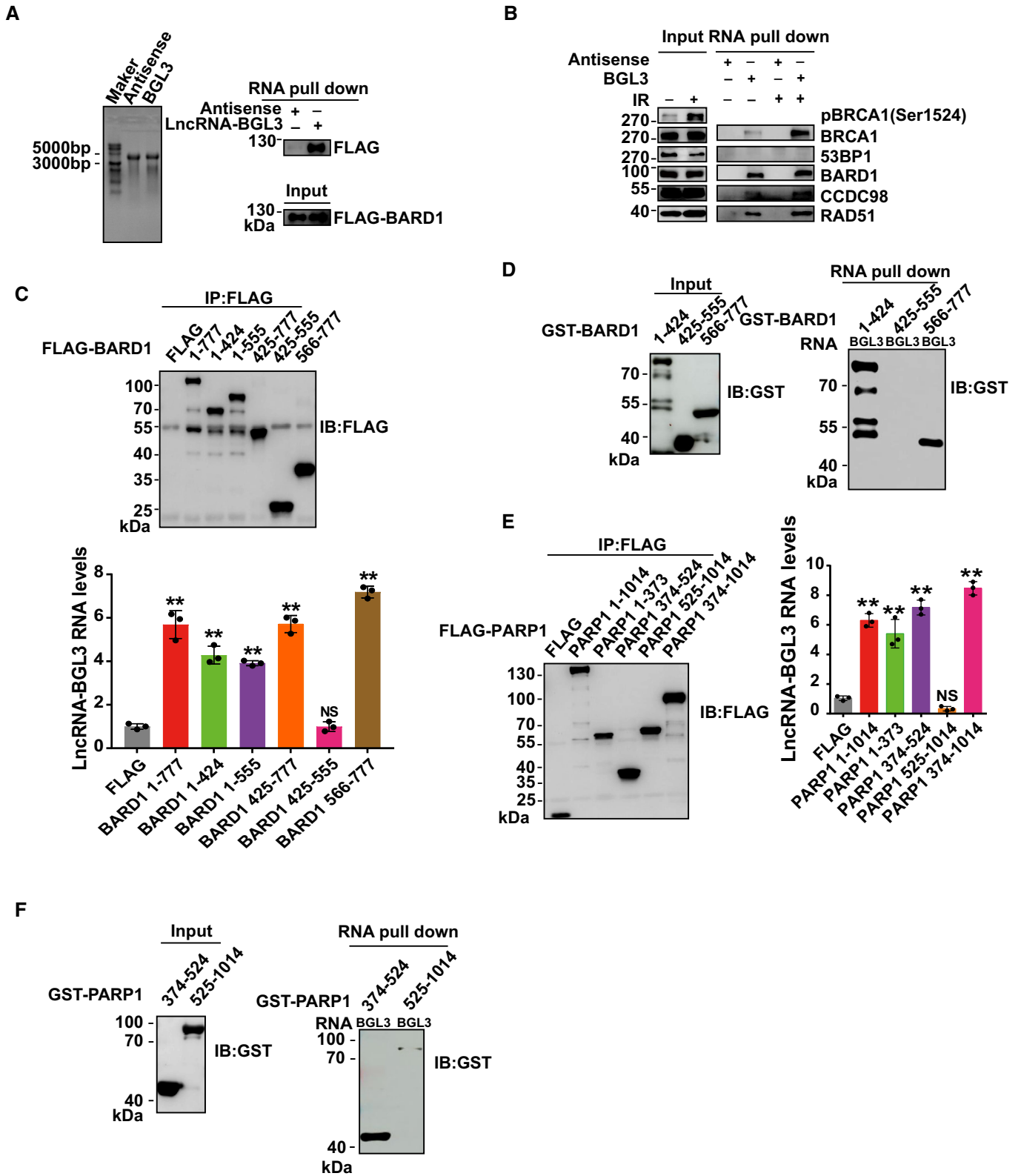


Figure EV2.

Figure EV2. Mapping the interaction regions between BGL3 and BARD1/PARP1.

- A BGL3 and antisense were transcribed *in vitro* and analyzed on an agarose gel. Ladder, 10 kb ssRNA ladder (left panel). FLAG-BARD1 was transfected into 293T cells. Forty-eight hours later, BGL3 RNA pull-down assays were performed. Samples were separated by sodium dodecyl sulfate (SDS) gel and blotted with indicated antibodies (right panel).
- B A non-denaturing pull-down assay for BGL3-BARD1 interaction. 293T cells were treated with or without IR (10 Gy) and recovered for 1 h. Biotinylated *in vitro*-transcribed lncRNA-BGL3 sense or antisense transcripts were incubated with cell lysates by non-denaturing lysis buffer, followed by Western blots using the indicated antibodies.
- C–F FLAG-tagged full-length or deletion mutants of BARD1 (C) or PARP1 (E) were transfected into 293T cells. BGL3 RNA immunoprecipitation assays were performed as described in the Materials and Methods. Data reported as the average of three independent experiments. Data are presented as mean \pm SD and analyzed by two-tailed Student's *t*-test, ***P* < 0.01, NS: no significant difference. GST-BARD1 (D) or PARP1 (F) deletion mutants were purified from *Escherichia coli*, and *in vitro* RNA pull-down assays were performed, as described in the Materials and Methods.

Source data are available online for this figure.

Figure EV3. BGL3 regulates DNA damage response.

- A U2OS cells transfected with or without FUGW-GFP-BARD1 were subjected to laser micro-irradiation to generate DSBs, and 10 min later, BGL3 and BARD1 recruitment was examined as described in the Materials and Methods.
- B U2OS cells were transfected with the indicated siRNAs, and BGL3 (RNA FISH) and γ H2AX (IF) recruitment to DNA damage sites was examined. Data shown are the average of three independent experiments (middle panel), and 100 cells were counted for each experiment, two-tailed Student's *t*-test, ***P* < 0.01. Knockdown efficiency of BGL3 siRNA was examined by qRT-PCR (right panel). Data are presented as mean \pm SD of three independent experiments, two-tailed Student's *t*-test, ***P* < 0.01.
- C RT-qPCRs to examine the BGL3 RNA levels of cytosolic, nuclear, and chromatin fractions before and following 6 Gy IR in 293T cells. Data are presented as mean \pm SD of three biological replicates, two-tailed Student's *t*-test, ***P* < 0.01.
- D HCT116 cells (left panel) and MDA-MB-231 cells (right panel) were treated as described in the Materials and Methods section, and cell response to ionizing radiation (IR) was analyzed by colony formation assays. Data are presented as mean \pm SEM of four independent experiments and analyzed by two-way analysis of variance (ANOVA), ***P* < 0.01.
- E HCT116 cells (left panel) and MDA-MB-231 cells (right panel) were transfected with the indicated siRNAs. Cell sensitivity to camptothecin (CPT), hydroxyurea (HU), etoposide (ETO), or IR was determined by MTS assays. Data were presented as mean \pm SD of three biological replicates. Two-tailed Student's *t*-test, ***P* < 0.01, NS: no significant difference.
- F BGL3 deficiency inhibits DNA damage repair. HCT116 cells (left panel) and MDA-MB-231 cells (right panel) were transfected with the indicated siRNA. Quantification of γ -H2AX foci at indicated times after irradiation (2 Gy) is presented. Data shown are results of three independent experiments (100 cells for each experiment), presented as mean \pm SD, and analyzed by two-tailed Student's *t*-test, ***P* < 0.01, NS: no significant difference.

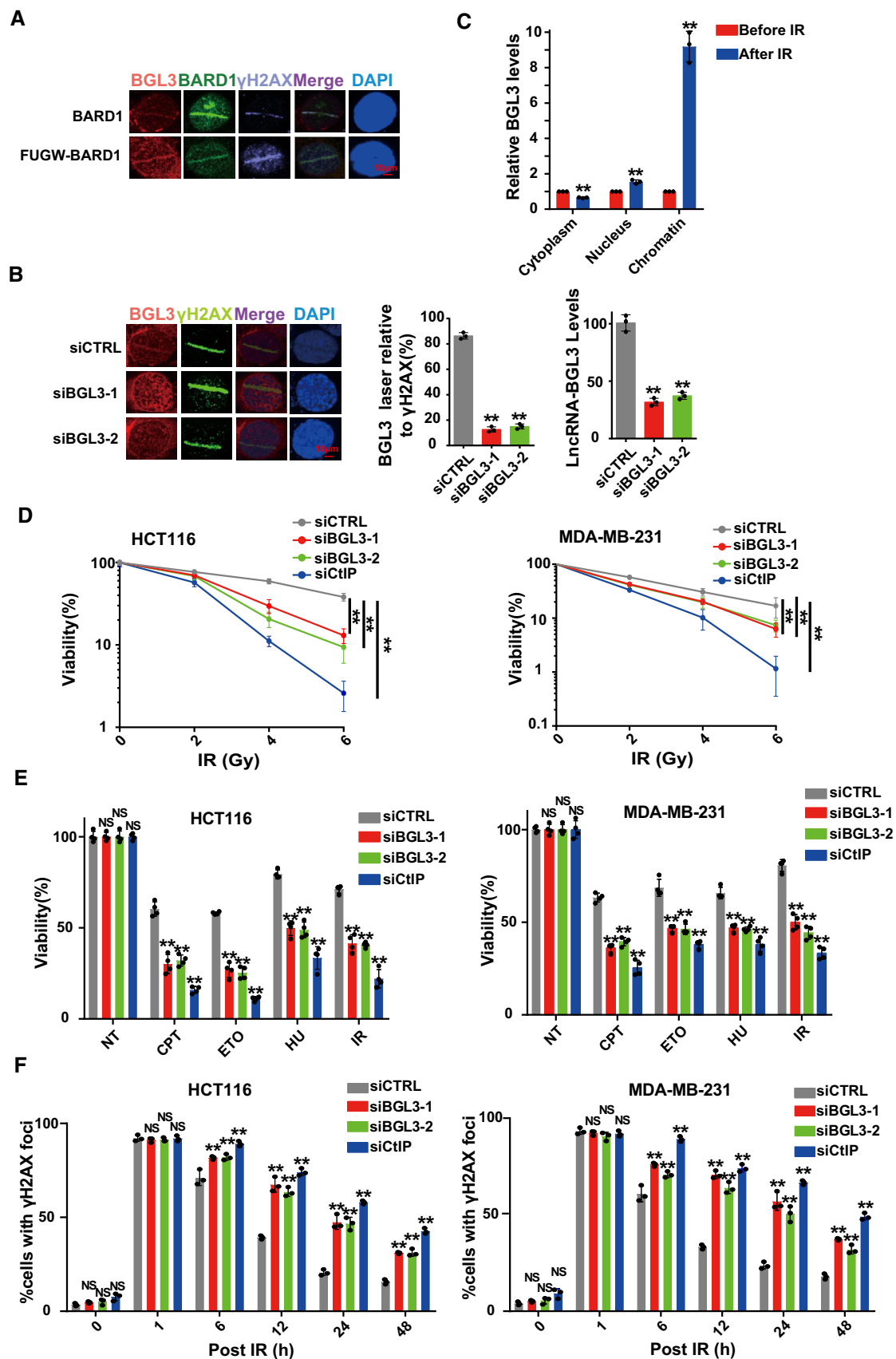


Figure EV3.

Figure EV4. BGL3 is required for HR.

- A MCF7 cells (upper panel) and MDA-MB-231 cells (lower panel) were transfected with the indicated siRNA, and 48 h later, cell responses to the PARP inhibitors veliparib (left panel) or olaparib (right panel) were measured by MTS assay. Data are presented as mean \pm SEM of three independent experiments and analyzed by two-way analysis of variance (ANOVA), $**P < 0.01$.
- B Cell cycle profile of wild-type or BGL3-depleted U2OS cells. Data shown are averages of three independent experiments, presented as mean \pm SD, NS: no significant difference.
- C Effects of BGL3 expression on cell growth. OD values of MCF7 cells expressing either control siRNA or different BGL3-specific siRNAs were monitored for 6 days. Data are presented as mean \pm SEM of four independent experiments and analyzed by two-way analysis of variance (ANOVA), NS: no significant difference.
- D MCF7 cells were transfected with the indicated siRNA. Quantification of dead cells at 12 h after irradiation (6 Gy) is presented. Data shown are results from three independent experiments, presented as mean \pm SD, and analyzed by two-tailed Student's *t*-test, $**P < 0.01$.

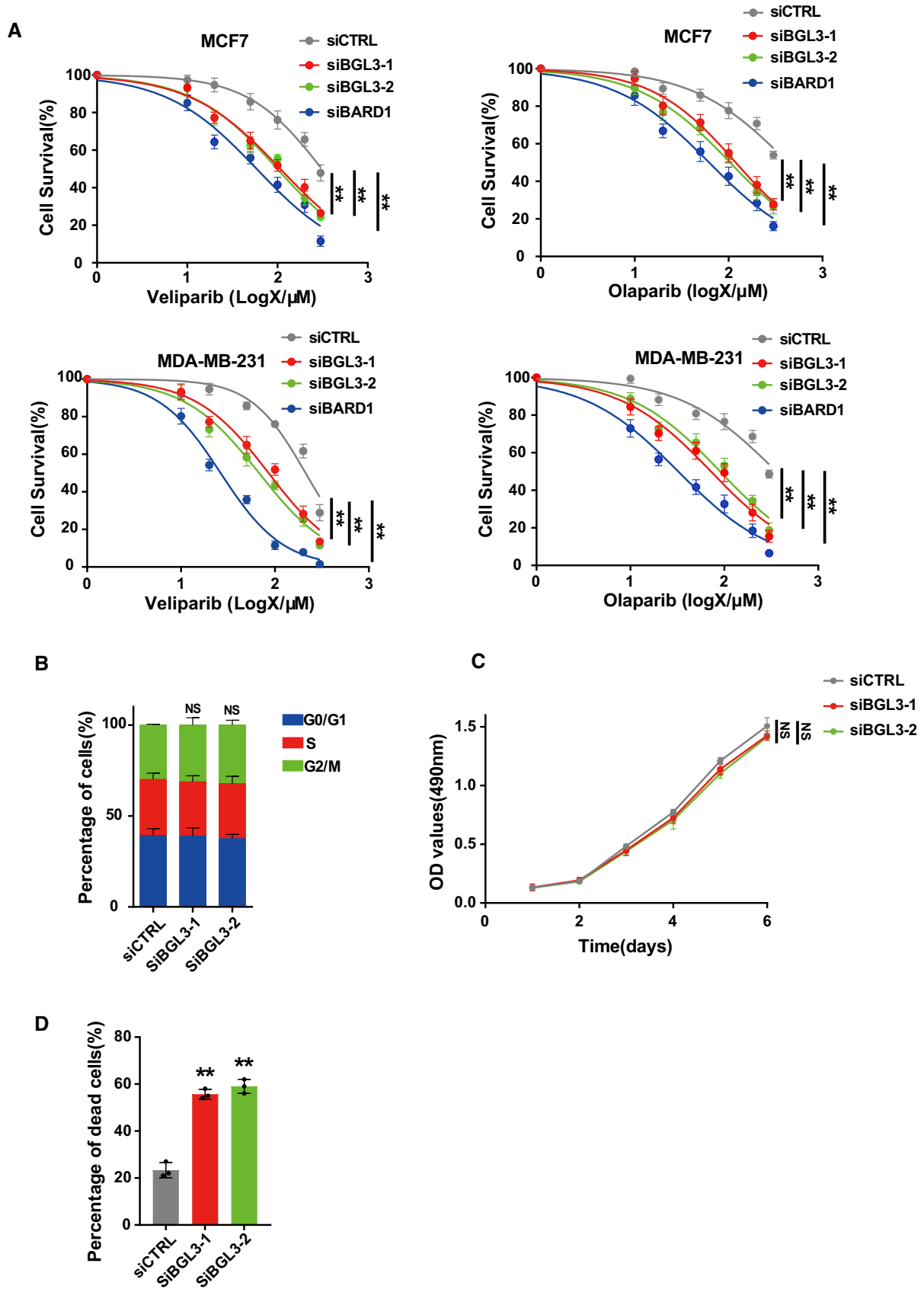


Figure EV4.

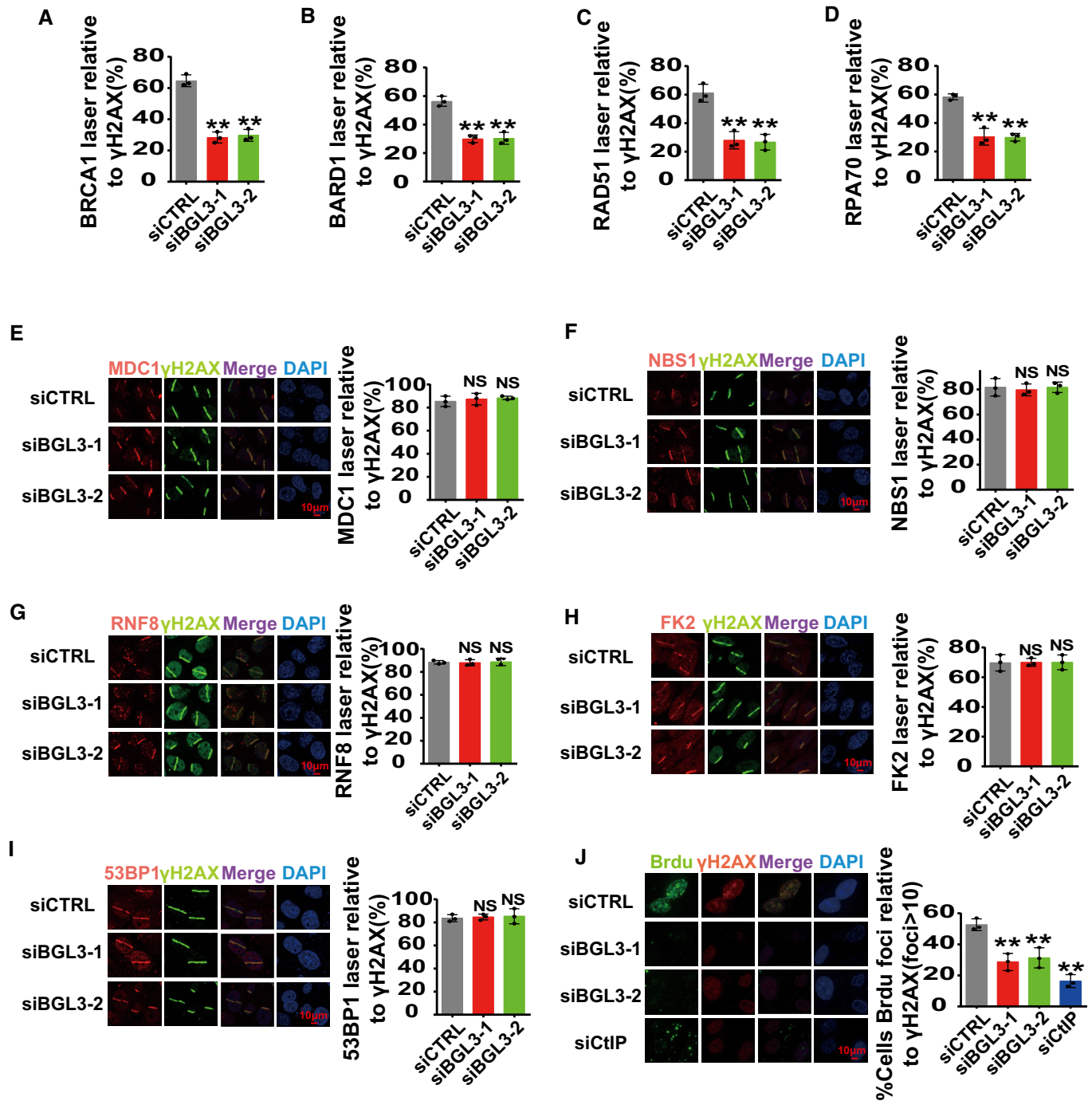


Figure EV5. BGL3 regulates BRCA1/BARD1 retention at DSBs.

A–D Quantification of Fig 3C–F. Data shown are the average of three independent experiments, and 100 cells were counted for each experiment. Data are presented as mean ± SD and analyzed by two-tailed Student's *t*-test, ***P* < 0.01, NS: no significant difference.

E–J Parental or BGL3-deficient U2OS cells were subjected to laser micro-irradiation to generate DSBs in a line pattern. DDR factor recruitment was examined 1 h later. Data shown are the average of three independent experiments, and 100 cells were counted for each experiment. Data are presented as mean ± SD and analyzed by two-tailed Student's *t*-test, ***P* < 0.01, NS: no significant difference.

Figure EV6. Both BGL3 and BARD1 function in HR.

- A U2OS cells were transfected with BGL3 or control siRNA, and BARD1 accumulation at sites of laser-induced DNA damage was examined at the indicated time points. Data shown are the average of three independent experiments, and 100 cells were counted for each experiment. Data are presented as mean \pm SD and analyzed by two-tailed Student's *t*-test, ***P* < 0.01, NS: no significant difference.
- B 293T cells were transfected with the indicated siRNAs, and cells were lysed. Samples were blotted with indicated antibodies (left panel). Knockdown efficiency of BGL3 siRNA was examined by qRT-PCR (right panel). Data shown are the average of three independent experiments, presented as mean \pm SD, and analyzed by two-tailed Student's *t*-test, ***P* < 0.01, NS: no significant difference.
- C BGL3 expression levels were examined by qRT-PCR at the indicated time points after irradiation (2 Gy). Data shown are the average of three independent experiments, presented as mean \pm SD, and analyzed by two-tailed Student's *t*-test, NS: no significant difference.

Source data are available online for this figure.

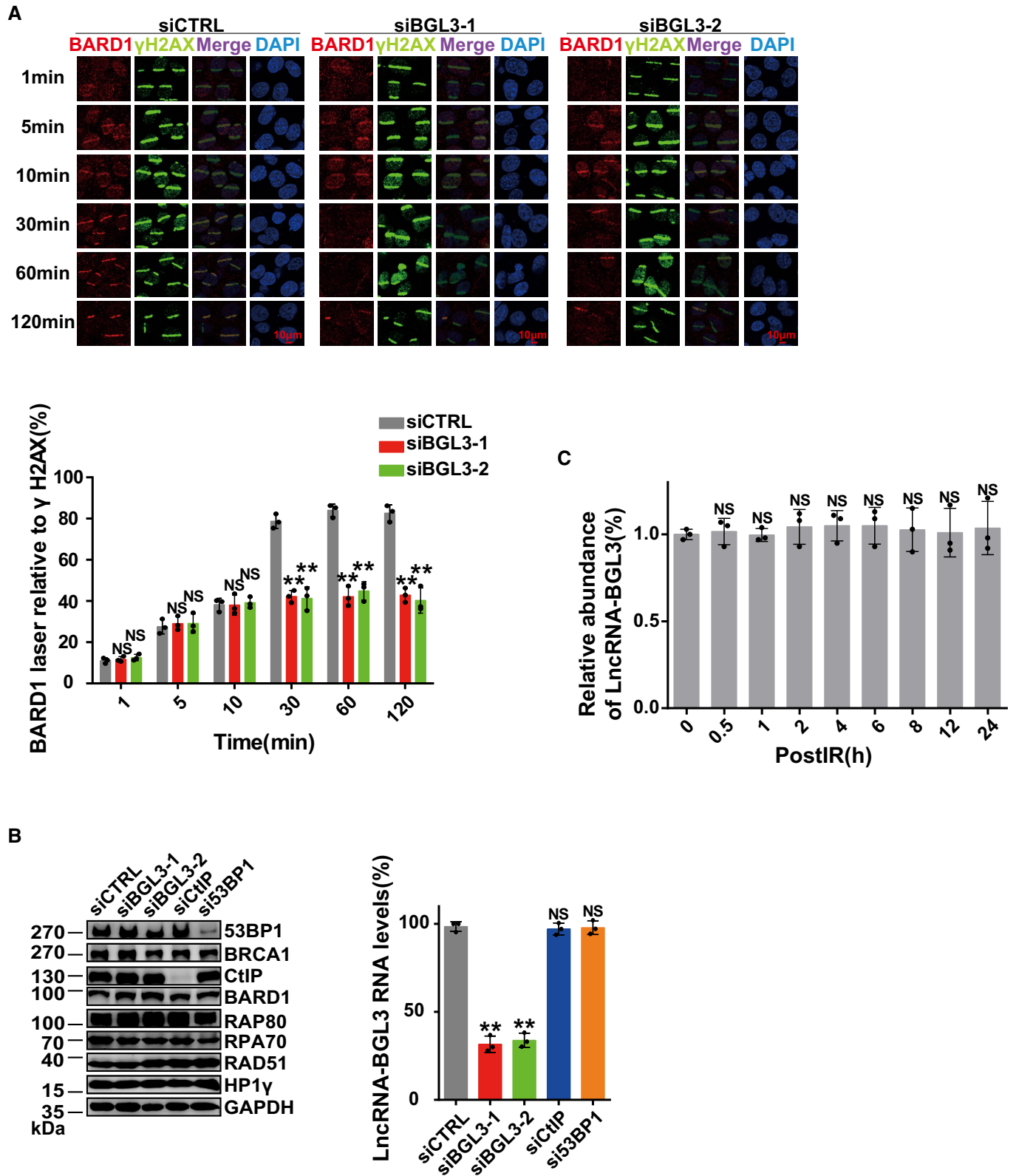


Figure EV6.

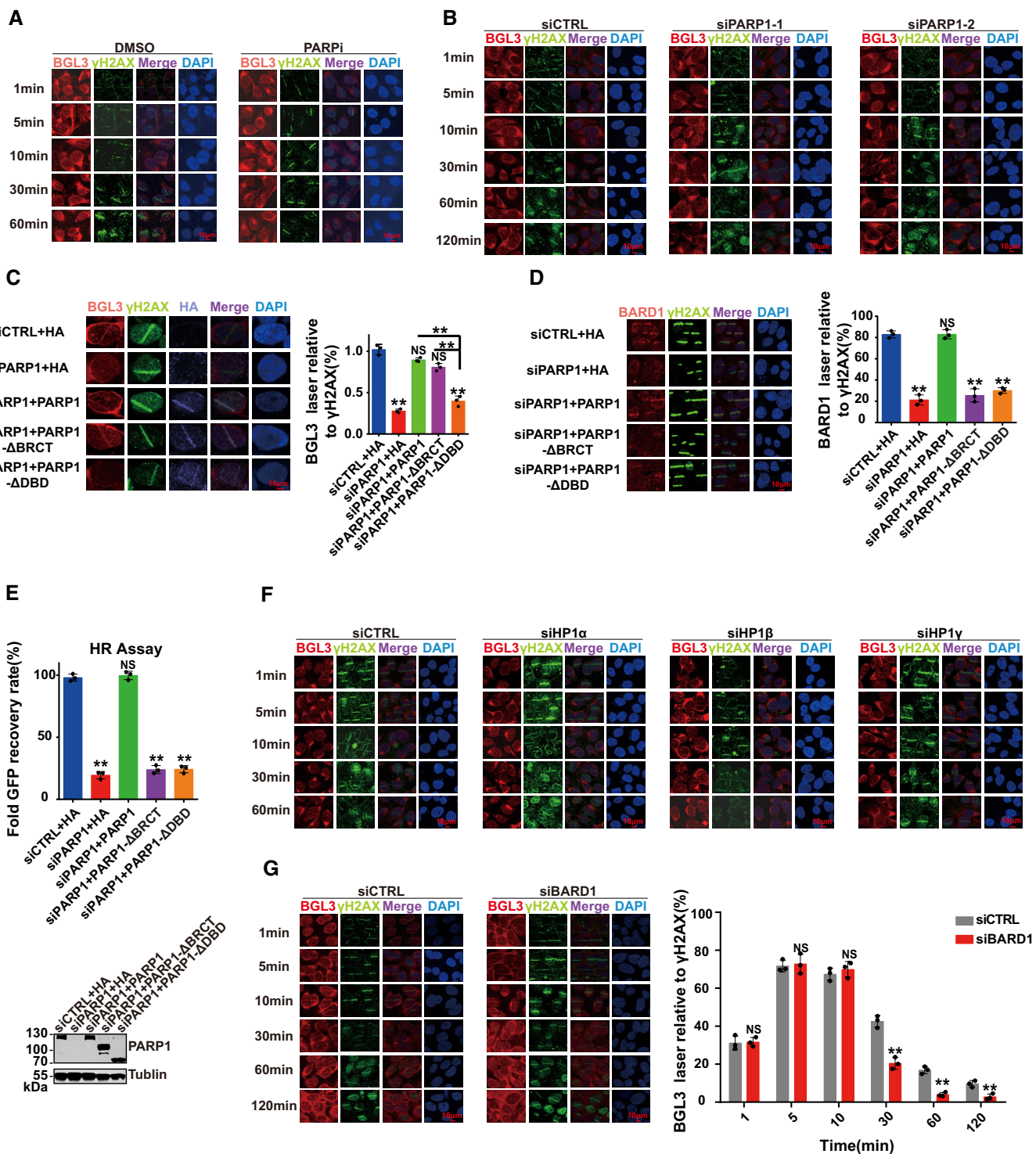


Figure EV7.

Figure EV7. PARP1 and HP1 γ affect BGL3 recruitment to DNA damage sites.

- A Representative micrographs of Fig 6C.
- B U2OS cells were transfected with indicated siRNAs, and BGL3 recruitment at the indicated time points was monitored.
- C U2OS cells were transfected with the indicated siRNAs or plasmids; then, BGL3 (RNA FISH) and γ H2AX (IF) were assessed following laser micro-irradiation and a 10-min recovery. Data shown are the average of three independent experiments, and 100 cells were counted for each experiment. Data are presented as mean \pm SD, $**P < 0.01$, NS: no significant difference.
- D U2OS cells were transfected with the indicated siRNAs or plasmids; then, BARD1 and γ -H2AX accumulation at sites of laser-induced DNA damage were examined. Data shown are the average of three independent experiments, and 100 cells were counted for each experiment. Data are presented as mean \pm SD, $**P < 0.01$, NS: no significant difference.
- E U2OS cells were transfected with the indicated siRNAs or plasmids, and the HR efficiency was determined using the reporter assay. Data are presented as mean \pm SD of three biological replicates, $**P < 0.01$, NS: no significant difference.
- F Representative micrographs of Fig 6D.
- G U2OS cells were transfected with BARD1 or control siRNA; then, BGL3 (RNA FISH) and γ H2AX (IF) accumulation at sites of laser-induced DNA damage was examined at the indicated time point. Quantification was average of three independent experiments, and 100 cells were counted for each experiment. Data are presented as mean \pm SD and analyzed by two-tailed Student's *t*-test, $**P < 0.01$, NS: no significant difference.

Source data are available online for this figure.